



TEST RIG DEDICATED FOR HARDWARE USED IN WIND TUNNELS

Aleksandra Ordon¹, Paulina Kurnyta-Mazurek²

¹ORCID: 0000-0001-6935-0605

²ORCID: 0000-0002-0938-0113

Faculty of Mechatronics, Armament and Aerospace,
Military University of Technology in Warsaw

Received 28 September 2021, accepted 12 December 2021, available online 12 December 2021.

Key words: wind tunnel measurement, servo-mechanism, LabVIEW software, myRIO controller.

Abstract

The paper presents the results of work on a measurement system dedicated to hardware used during wind tunnel tests, especially to servomechanisms. These devices could be applied to set a specific position of the control surface. The proposed system would ensure continuous monitoring of servo-rotor position and servo-motor temperature and would avoid uncontrolled change of control surface position.

The application designed to monitor the operating status of the servomechanism was prepared in the LabVIEW software and was implemented on the myRIO platform. The developed test rig allows to register time histories of servo-rotor position and temperature during test for different values of applied load. In the paper, studies planned were also presented.

Experimental studies show that before wind tunnel tests, selected servomechanism should be tested in terms of maintaining the parameters declared by the manufacturer, especially during continuous operation. The developed measurement system can be used during wind tunnel tests, as well as only for servo-mechanism parameter testing.

Correspondence: Paulina Kurnyta-Mazurek, Zakład Awioniki, Instytut Techniki Lotniczej, Wydział Mechatroniki, Uzbrojenia i Lotnictwa, Wojskowa Akademia Techniczna, 00-908 Warszawa, e-mail: paulina.mazurek@wat.edu.pl; aleksandra.ordon@student.wat.edu.pl.

Introduction

Wind and water tunnel measurements play an important role in aircraft research programmes, due to the cost minimalization and time saving (BARLOW et al. 1999, Operations and Maintenance Manual 2012). These tests are one of the experimental method (LICHON et al. 2016), which allow to verify the characteristics obtained during computer studies performed in specialized software with use of numerical methods presented for example in (PANDYA et al. 2017, LI et al. 2018). Moreover, wind tunnel measurements provide the opportunity to studies of new solutions dedicated to aircrafts, before tests in flight, such as fault detection system described in (RUANGWISSET, SUWANTRAGUL 2008). Also in the paper (WIBOWO et al. 2019) comparison of aerodynamic characteristics of Sukhoi SU-33 aircraft and F-35 Lightning aircraft obtained in wind tunnels are presented.

Wind tunnel measurements allow to simulation of the aircraft real behavior in strictly defined conditions and with precisely set flight parameters. These tests enable to eliminate errors and improve of aircraft operating parameters at the design stage, as well as detect causes of failures that occurred in the air. In comparison with tests in flight, tunnel measurements possess several attractive advantages, such as reducing research time and costs.

For tunnel test, aircraft models in appropriate scale were made. These models were often prepared with use of method, which is very popular in engineering, namely 3D printing (MALEK et al. 2019, KIŃSKI, SOBIESKI 2020, RAZA et al. 2021). During tests, the control surfaces such as ailerons, elevator and rudder were locked in strictly defined position. Despite significant progress already reached in wind and water tunnel measurements, there remain numerous open challenges in this field. Sometimes, due to mounting errors or excessive load, the control surfaces change their position. For that reason, in the paper we proposed the use of servomechanism with dedicated measurement system to ensure continuous monitoring of servo-rotor position and servo-motor temperature. Designed system can be used during wind tunnel tests, as well as only for servo-mechanism parameter testing.

The contents of the paper are organized as follows. First section introduces servomechanism, considering their structures and operation principle. Second section reports on laboratory test stands, especially measurement system and developed algorithm. Afterwards, results in form of time histories of the measurement system are presented. Finally, some remarks are presented in Conclusion Section.

Servomechanisms in aircraft models

Remote control servomechanism (RC servo) are devices designed specifically for pointerlike position-control applications. They are built of dc motor, feedback device and control circuit. An RC servo uses an outside pulse-width-modulated (PWM) signal to control the position of its shaft. To change the position of the shaft, the pulse width of the modulated signal is varied. To make the shaft go counterclockwise from neutral position, a pulse wider than 1.5 ms is applied to the control input. Conversely, to make the shaft go clockwise, a pulse narrower than 1.5 ms is applied. The shaft of the motor is usually limited to a rotation of 180° or 210° . The dependence between the servo arm position and the length of the supplied control impulse signal is shown in Figure 1.

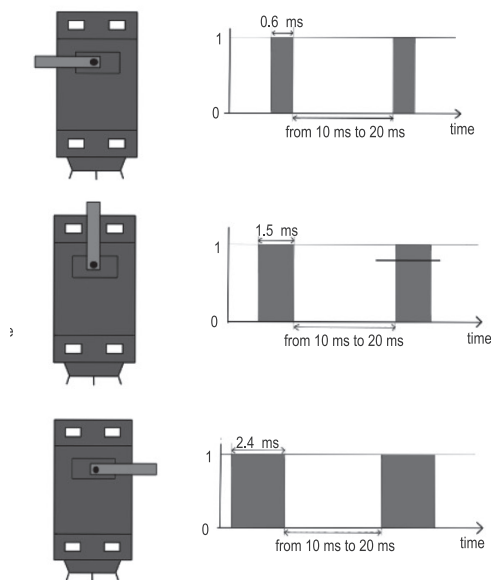


Fig. 1. The dependence between servo arm position and the length of the supplied control pulse signal

Servomechanisms in models airplanes are designed to precisely control the deflection of control surfaces, such as ailerons, flaps or rudder. Furthermore, they are used in landing gear extension mechanisms in unmanned aerial vehicles. They are also responsible for changes in the angle of attack of the rotor blades, as well as the pitch of the tail rotor in helicopter models (STEPHEN et al. 2011). Figure 2a shows a example of servomechanism and Figure 2b shows a fragment of the interior of the fuselage with marked servos in charge of controlling the rudder, elevator and throttle.

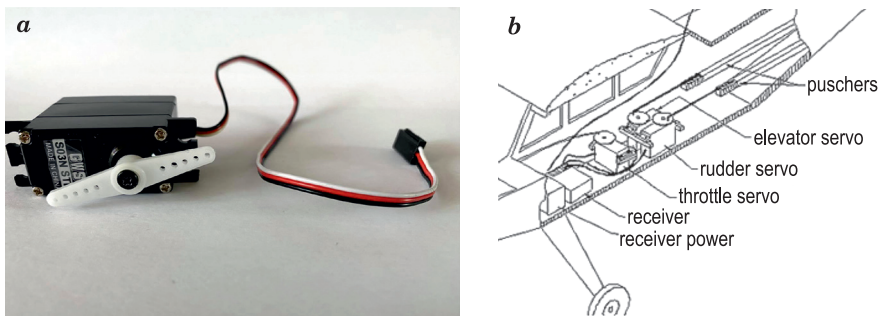


Fig. 2. Photo of the servomechanism GWS S0SN STD (a) and fragment of the interior of the fuselage (b)

In the Figure 3 servo control system was presented. When controlling servos within model airplanes, an initial control signal is first sent to a radiowave modulator circuit that encodes the control signal within a carrier wave. This carrier wave is then radiated off as a radiowave by an antenna and transmitted to the receiver circuit model. The receiver circuit recovers the initial control signal by demodulating the carrier. After that, the control signal is sent to the designated servo within the model and its arm is tilted by the specified angle.

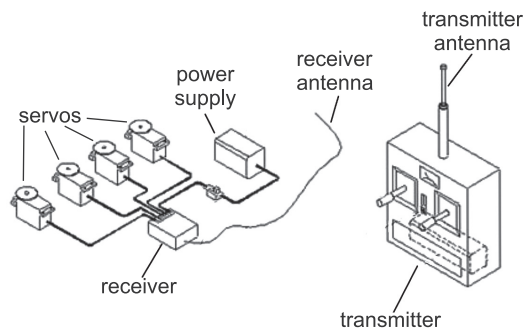


Fig. 3. Diagram of the four-channel control system of the flying model

If there is more than one servo per model, more channels are required. For example, most RC airplanes require a four-channel radio set. More complex models may use five or six channels to control additional features such as flaps and retractable landing gear. The main control channels of airplanes RC models include:

- throttle control channel;
- elevator control channel;
- aileron control channel;
- rudder control channel.

The first mentioned control channel comprises throttle position adjustment. It is responsible for controlling the number of engine revolutions per minute. It can be controlled using a single servo. In the case of internal combustion engines, the throttle regulates the amount of air-fuel mixture supplied to the combustion chamber. In the case of airplanes with an electric motor, it is not used because the engine speed is controlled by changing the value of the voltage supplied to the engine.

Another mentioned steering channel allows to adjust the position of the elevator. With its help, the pilot can change the flight path, angle of attack α and side slip angle β .

The third control channel allows to control the deflection of the ailerons. These control surface make possible to change the roll angle Θ of the plane, therefore they allow to make a turn, and even a rotation around the longitudinal axis of the plane (Ox). Their position is changed by the movement of the control stick right-left or by the movement of the steering wheel in the appropriate direction. The aileron action changes the lifts on the wing.

The last mentioned control channel enables the control of the rudder position, which allows to initiate the rotation of the airplane about the vertical axis Oz . When its position is properly synchronized with the ailerons, it contributes to the correct execution of the turn.

Test rig

The motivation for the implementation of this type of test rig is the need to verify the parameters of servomechanisms given by manufacturers in the catalog notes of devices that can be used in models used in tunnel tests. We additionally propose the use of the developed system in tunnel tests during the operation of the airframe surfaces of an airplane model. The observed and registered parameters of servomechanism are the angular position of the servo drive shaft and the temperature of the servo housing. To monitor the above-mentioned parameters, measurement system with potentiometer and temperature sensor were designed and manufactured (GÜNTER et al. 2006). The scheme of the rig stand is shown in Figure 4.

The myRIO device was used as a control unit in the designed test rig. In turn, the application managing the stand was made in the LabVIEW software due to the compatibility of this environment with the myRIO device. A potentiometer was used to perform the task related to the monitoring of the angular position of the servo shaft, while a resistance temperature sensor was used to measure the temperature, due to its high sensitivity even with small changes in temperature. An ammeter has been attached to the system, which gives information about the intensity of the current consumed by the servo. The stand base was designed in the SolidWorks program, and then printed with using a 3D printer.

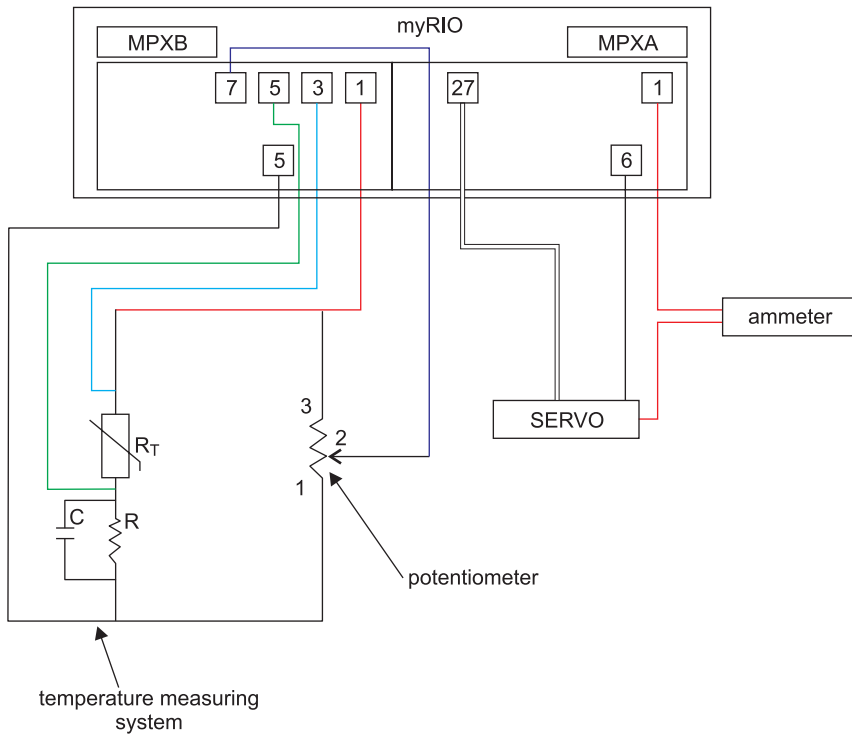


Fig. 4. Scheme of the test rig

The myRIO device in the designed laboratory stand acts as a control unit. It is a portable, configurable device that enables, among other things, the design of control systems and measurement applications. It is equipped with a powerful Cortex-A9 dual-core processor, Real Time System and FPGA (Field Programmable Gate Array). All elements of the system can be configured using applications prepared in the LabVIEW software. There are two expansion ports MPX A and MPX B at the user's disposal, led out to double-row 34-vertical connectors. The location of the connectors is identical in both ports, and their numbers along with the function performed are shown in Figure 4.

The test rig uses a temperature sensor, which is designed to monitor the temperature of the servo housing during operation with a load set by the user. It is a resistance sensor where the sensitive element is a thermistor with a negative temperature coefficient – NTC (Negative temperature coefficient). In this type of resistor, the resistance decreases with increasing temperature. The relationship between the resistance and the temperature in an NTC thermistor is described by the following equation which has been obtained from the datasheet:

$$T = \frac{1}{\frac{1}{T_0} + \frac{1}{\beta} \ln\left(\frac{R_T}{R_0}\right)} \quad (1)$$

where:

R_T – the sensor resistance at a given temperature,

R_0 – the sensor resistance at the reference temperature,

T – the sensor temperature at the time of measurement,

T_0 – the sensor reference temperature.

The symbol β means a constant that is provided by the manufacturer in the data sheet. In order to use the described sensor (thermistor) to measure the temperature of the servo, a specified measuring system should be built, which will consist of a resistor, sensor and a capacitor. Placing a thermistor in the upper branch of the voltage divider makes the voltage measurement more accurate. According to the catalog note of the NTC sensor, its accuracy of resistance measurement is 1% with increasing temperature. The temperature measuring system is shown in Figure 5.

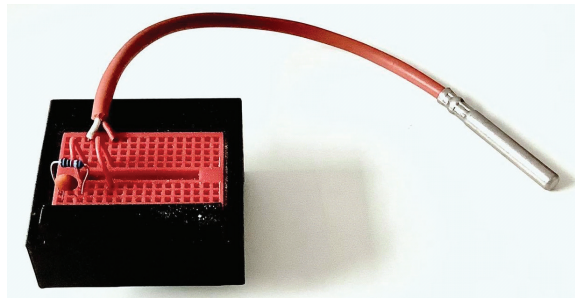


Fig. 5. Temperature measuring system

A potentiometer is a sensitive element in the system designed to monitor the position of the servo shaft, and thus also its horn. This measurement is especially important when testing the maximum time for which a given load is maintained as well as in monitoring the correctness of the control surfaces deflection of an airplane model during tunnel tests. In order to obtain greater accuracy of measuring the angular position of the towing bar and to facilitate the assembly at the stand, the potentiometer has a cap, designed and printed in a 3D printer. The potentiometer with the cap on is shown in Figure 6.

The potentiometer is connected to the servo shaft by means of a belt drive-like mechanism. All gear elements, i.e. potentiometer cover, servo shaft cover, as well as a rubber strip were designed in the SolidWorks program and printed in a 3D printer. With each movement of the servo shaft, the potentiometer knob sets in motion. The system for monitoring the position of the servo shaft is shown in Figure 7.

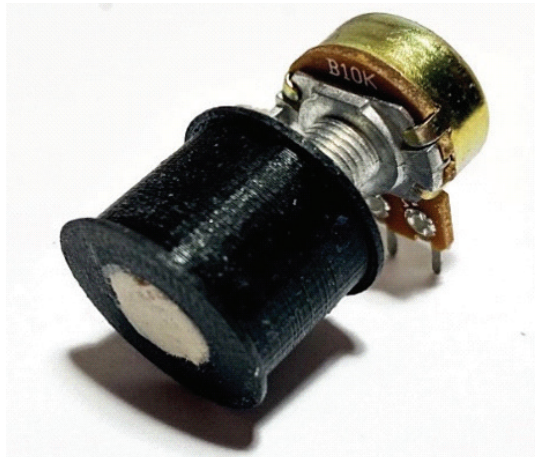


Fig. 6. Potentiometer with the cap

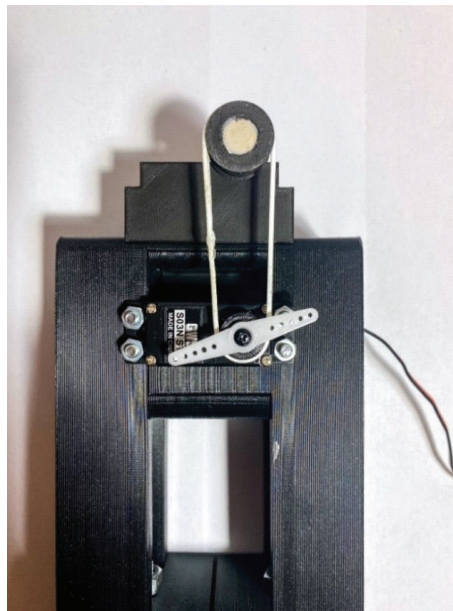


Fig. 7. Connection of a potentiometer with a servo

In order to enable the percentage assessment of the servo shaft position change, for each tested device, the difference in the potentiometer indications in its two extreme positions was calculated, which was divided into 100% of the range. When analysing the time courses, it should be assumed that a 1% change of the servo shaft position corresponds to a different value for each device.

For the servo GWS SO3N it is 0.03 V/%, for the Power HD 3001 HB it is 0.018 V/% and for the Power HD 6001 HB it is 0.027 V/%. The accuracy of reading the data from the potentiometer is 0.001 V. Due to the fact that the voltage change was converted into a percentage change of the shaft position, it was assumed that the measurements of the shaft position change were made with an accuracy of 0.1%.

The control and measurement application of the test rig was developed in the LabVIEW software. The prepared application is designed to control the angular position of the servo drive using the PWM signal, as well as receive data from the potentiometer and temperature sensor. The user interface of the developed application is presented in Figure 8.

The application has been divided into parts carrying out specific tasks. The servomechanism control section is marked by red line, the part showing the measurement results from the temperature sensor is blue. On the other hand, the fields on which the current voltage value from the potentiometer and the time history of the output voltage value from the potentiometer are displayed are marked by green line. Yellow is the color of the operating mode selection menu, by means of which the temperature sensor or potentiometer mode could be selected. Additionally, the user can stop the test (experiment) at any time and decide to save the data from the temperature sensor and potentiometer to a text file using the buttons in the menu (marked in purple). In the workstation selection section, it is possible to check status of individual systems, i.e., the position verification system and the temperature monitoring system. During operation in the "Measuring station" mode, it is possible to monitor the temperature, the position of the servo horn, control the servomechanism, and also save the measurement data to a text file. The application has protection against excessive heating of the housing of the tested servo. After exceeding the maximum operating temperature, the diode next to the thermometer starts to glow red.

The *Case* structure window that performs this task is shown in Figure 9. The part responsible for controlling the tested servo is marked in red, the measuring part responsible for reading the measurement parameters from the temperature sensor and potentiometer is marked in green, and the structure that records the measurement data to a file is marked by blue line. *While Loop*, in which the servo control task is performed, is executed every 10 ms. The tasks performed by the temperature sensor and the shaft position sensor of the servomotor are placed in the *While loop*. The *Wait* function is assigned a fixed value of 1 s. This means that the program waits a second between successive executions of the loop. Due to the fact that these components are placed in a separate structure, it is possible to disable their operation without interfering with the servo control. The sampling time values can be modified as needed. If we want to acquire data more frequently, we can reduce the value of the sampling time.

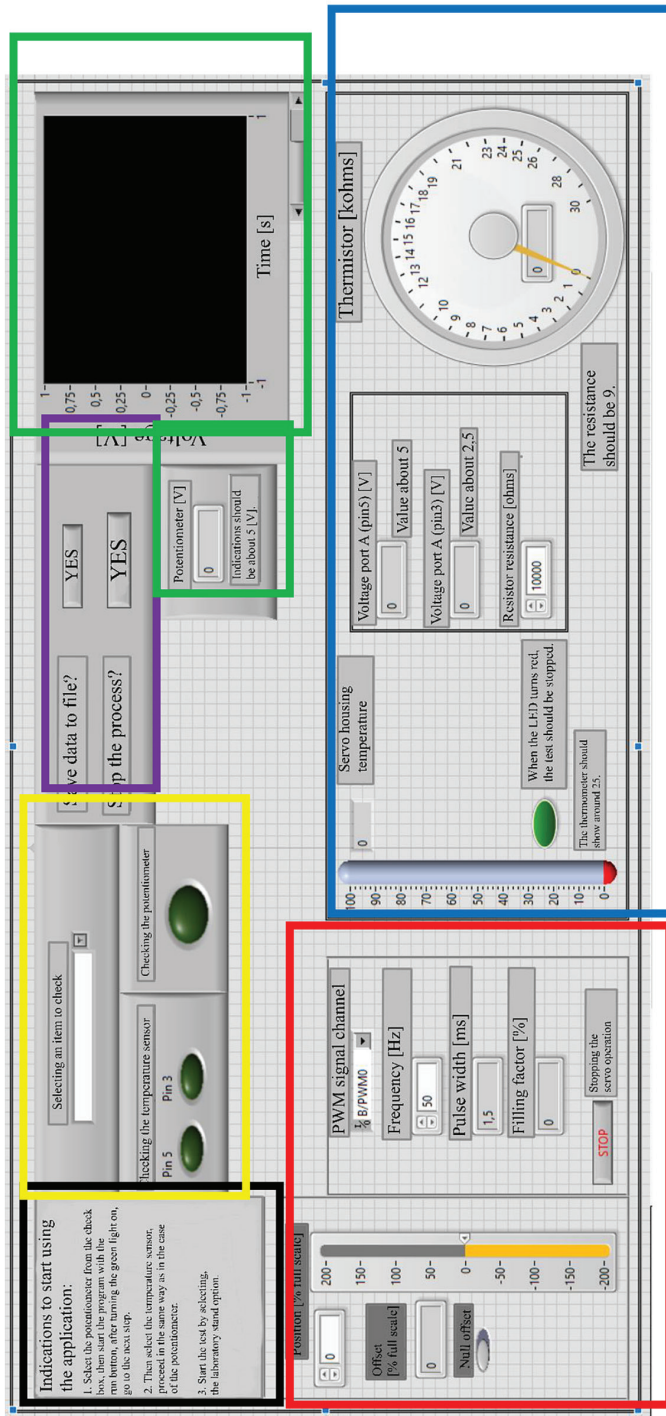


Fig. 8. Application interface

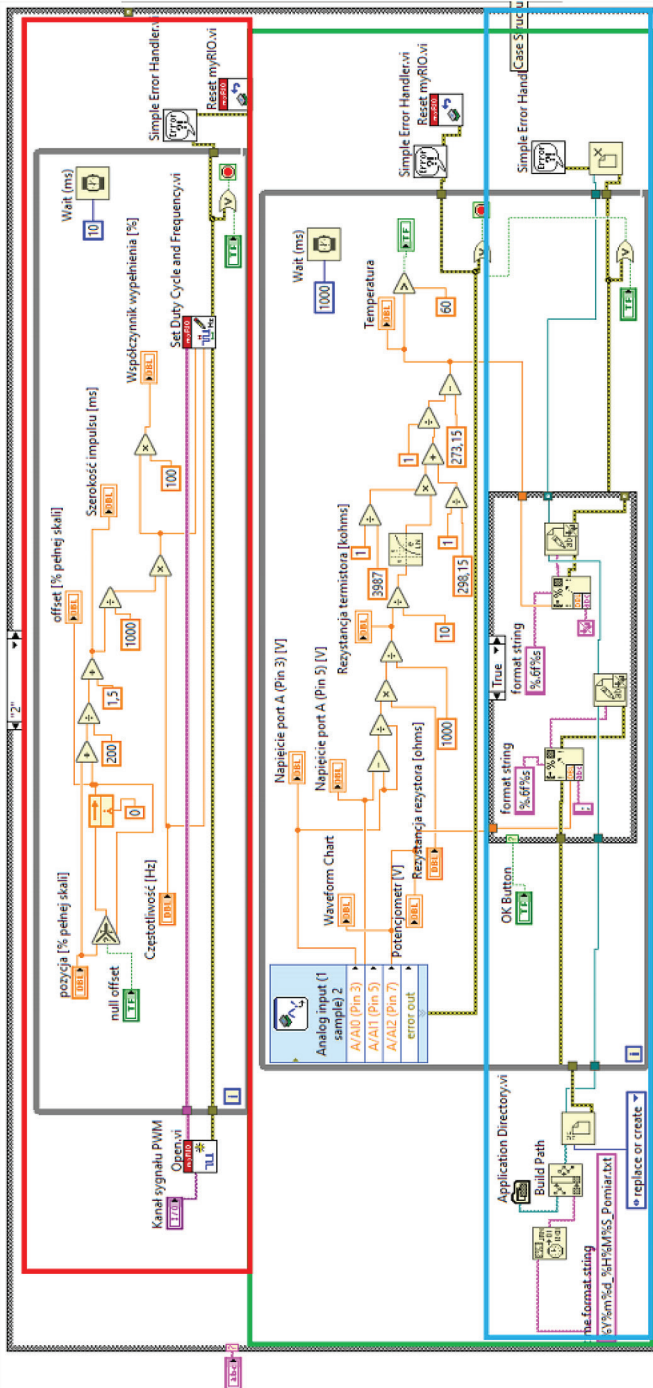


Fig. 9. Workstation structure window

Results and discussion

In order to verify the correct operation of the designed test stand, four measurement sessions were carried out for three different servos. The first one was a device dedicated to work with the myRIO platform (GWS S03N STD). Two another ones had designation Power HD 3001 HB and a Power HD 6001 HB, respectively. Their common feature is dimensions, they all belong to the standard category. For each research session, time history of the output voltage value from

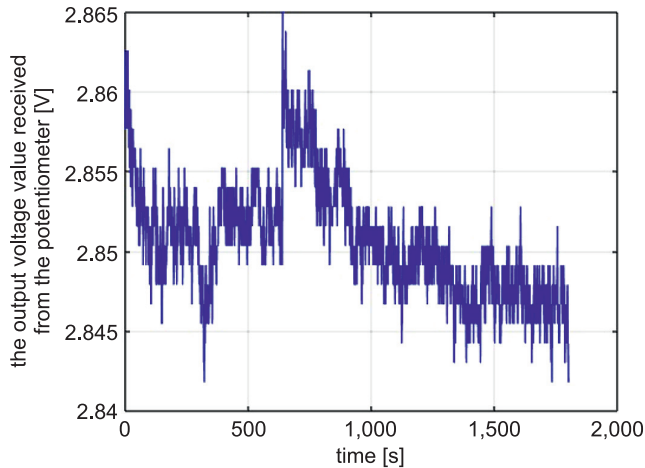


Fig. 10. Time history of the output voltage received from the potentiometer for 100% of the maximum load

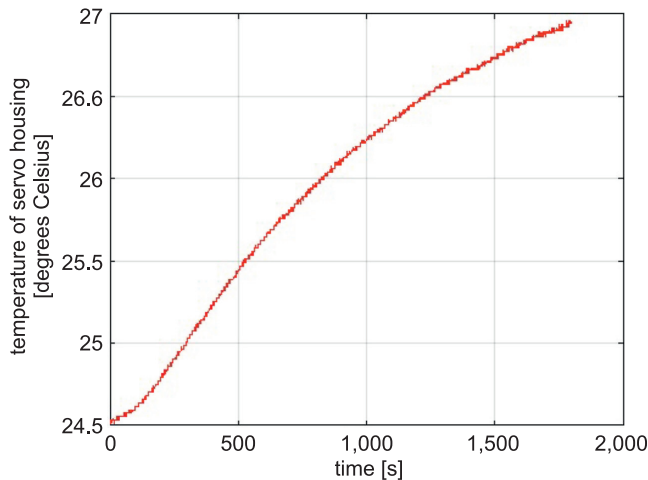


Fig. 11. The time history of the housing temperature of the tested servo, for 100% of the maximum load

the potentiometer were recorded, which determine the angular displacement of the actuator shaft and the time history of the device housing temperature were saved in text file too. Additionally, during the experiments, the intensity of the current consumed by the servo from the power source was examined. The duration of each experiment was 30 minutes, due to the fact that this is the maximum duration of the study in wind tunnels for a given position of the control surface. Each research experiment was divided into five stages, in which the load applied to the servo was 10, 30, 50, 70 and 100% of the maximum load, respectively. For each measurement, an appropriate mass in the form of a weight was suspended on the arm of the mechanism, 2 centimetres from the shaft center of the device. The values of individual loads for all devices are presented in Table 1.

Table 1

Values of servo loads

	GWS S03 STD [kg]	POWER HD 3001 HD [kg]	POWER HD 6001 HD [kg]
10% of maximum load	0.170	0.175	0.290
30% of maximum load	0.510	0.525	0.870
50% of maximum load	0.850	0.875	1.450
70% of maximum load	1.190	1.225	2.030
100% of maximum load	1.700	1.750	2.900

Time histories were recorded for each servo. Time histories of potentiometer output voltage and temperature of the GWS S03N STD servo for 100% load are shown in Figures 10 and 11.

Figure 12 shows the percentage change in the angular position of all tested servos depending on the load. The best operating parameters have a servo-mechanism dedicated to myRIO with the designation GWS S03N STD, which

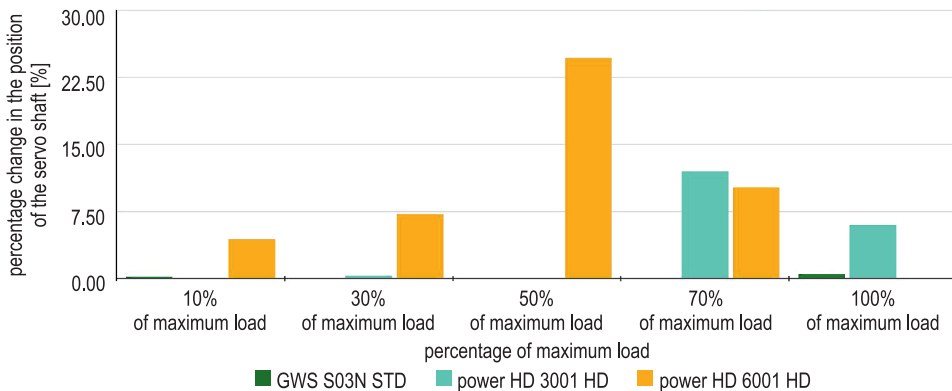


Fig. 12. Comparison of the percentage change in the angular position of the servo shaft during operation

maintained a given position during operation under each given load. The servomechanism with similar operating parameters, designated as POWER HD 3001 HB, did not maintain its position at the load equal to 70 and 100% of the maximum load. The last tested servo POWER HD 6001 HD did not maintain the set position under any load.

Analysing the above graph, it can be concluded that in the last stage of the tests, it should not be assumed that the device will maintain the set load, because it may have a manufacturing defect, similar to the most likely recently tested device, which did not meet its operating parameters.

Conclusion

In the paper, we proposed measurement system dedicated to hardware used during wind tunnel tests, especially to servomechanisms. These measurements are a one of experimental methods in the aircraft research programme, which let to obtaining the full range of data needed to guide detailed design decisions for many practical engineering problems.

In order to reduce the costs of the design and research of the aircraft system, in our work, we propose the use of servos both in tunnel tests and in flight test. In that case, detailed servomechanism test should be performed, especially its data sheet parameters should be studied. For that reason, test rig were designed and made.

The test rig is very universal and its operation is very intuitive, therefore it enables the testing of operating parameters and monitor of the servomechanisms operation. This is especially useful in tunnel tests where the control surfaces of the model are deflected and the servo shafts are loaded throughout the test. Hence, it is justified to perform tests of servomechanisms before using them in tunnel tests. Thanks to them, it is possible to eliminate the error related to the servo not maintaining the set position or excessive heating of the housing. The data presented in the previous chapter show that not all devices maintain the load declared by the manufacturer. The servo was tested and it probably had a manufacturing defect. Conducting the tests on the prepared stand made it possible to quickly identify it and reject it for later use in tunnel tests.

References

- BARLOW J.B., RAE W.H., POPE A. 1999. *Low-Speed Wind Tunnel Testing*. 3rd Ed., Wiley, Hoboken.
- HOMMEL G., HUANYE S. 2006. *Embedded Systems – Modeling, Technology, and Applications*. Springer Netherlands, Amsterdam.
- KIŃSKI W., SOBIESKI W. 2020. *Geometry extraction from GCODE files destined for 3D printers*. Technical Science, 23(2): 1-16. <https://doi.org/https://doi.org/10.31648/ts.5644>.

- LI S., NIU X., HUANG X. 2018. *Study on the correlation between the dynamic test of airfoil wind tunnel and CFD calculation*. CSAA/IET International Conference on Aircraft Utility Systems (AUS 2018), p. 62-66. <https://doi.org/10.1049/cp.2018.0263>.
- LICHOŃ D., MIKOŁAJCZYK A., KISZKOWIAK Ł., ŁĄCKI T. 2016. *Identification of UAV static aerodynamic characteristics in the water tunnel balance research*. Zeszyty Naukowe Politechniki Rzeszowskiej, 293, Mechanika 88RUTMech., XXXIII, 88 (2): 127-140.
- MAŁEK E., MIEDZIŃSKA D., POPLAWSKI A., SZYMCZYK W. 2019. *Application of 3d printing technology for mechanical properties study of the photopolymer resin used to print porous structures*. Technical Science, 22(2): 183-194.
- Operations and Maintenance Manual. 2012. Model 2436 Flow Visualization Water Tunnel, Rolling Hills Research Corporation. References.
- PANDYA Y., SREEVANSU Y.G., SHARMA A., JAIN K., JENA S., PAWAR A.A., RANJAN K.S., SAHA S. 2017. *Aerodynamic characterization of a model aircraft using wind-tunnel testing and numerical simulations*. First International Conference on Recent Advances in Aerospace Engineering (ICRAAE), p. 1-6. <https://doi.org/10.1109/ICRAAE.2017.8297239>.
- RAZA A., FARHAN S., NASIR S., SALAMAT S. 2021. *Applicability of 3D Printed Fighter Aircraft Model for Subsonic Wind Tunnel*. International Bhurban Conference on Applied Sciences and Technologies (IBCAST), p. 730-735. <https://doi.org/10.1109/IBCAST51254.2021.9393214>.
- RUANGWISET A., SUWANTRAGUL B. 2008. *Wind tunnel test of UAV fault detection using principal component based aerodynamic model*. IEEE International Conference on Mechatronics and Automation, p. 150-154. <https://doi.org/10.1109/ICMA.2008.4798742>.
- TOBIN S.M. 2010. *DC Servos: Application and Design with MATLAB*. CRC Press Inc., Boca Raton.
- WIBOWO S.B., FAJAR M., NAUFAL W.F., SINURAT D.F., SUTRISNO I., BASUKI B. 2019. *Comparison of Aerodynamic Characteristics on Sukhoi SU-33-like and F-35 Lightning II-like Models using Water Tunnel Flow Visualization Technique*. 5th International Conference on Science and Technology (ICST), p. 1-6. <https://doi.org/10.1109/ICST47872.2019.9166275>.